Colourless *p*-phenylene-spaced bis-azoles for luminescent concentrators

Chiara Manzini,[a] *Giulia Marianetti,*[b] *Cristofer Pezzetta*[a,b] *Elisabetta Fanizza,*[c,d] *Marco Lessi,*[a] *Pierpaolo Minei,*[a] *Vincenzo Barone,*[b] *Fabio Bellina,*[a,e] *Andrea Pucci*[a,e,*]

(a) Dipartimento di Chimica e Chimica Industriale, Università di Pisa, Via Moruzzi 13, 56124 Pisa, Italy
(b) Scuola Normale Superiore, Piazza dei Cavalieri 7, 56126 Pisa (Italy)
(c) Dipartimento di Chimica, Università degli Studi di Bari, Via Orabona 4, 70126 Bari, Italy
(d) CNR-Istituto per i Processi Chimico Fisici, UOS Bari, Via Orabona 4, 70126 Bari, Italy
(e) INSTM, UdR Pisa, Via Moruzzi 13, 56124 Pisa, Italy
* Corresponding author: andrea.pucci@unipi.it;

Abstract

We report on the synthesis of new push-pull imidazole-benzothiazole and thiazole-benzothiazole fluorophores obtained in good yields by using direct C-H arylation synthetic strategies. Spectroscopic investigations in $CHCl_3$ solution evidenced that the 1,4-phenylene-spaced imidazole-benzothiazole composed by an electron-donating dimethylamino group achieved a trade-off between fluorescence maximum (516 nm), Stokes shift (165 nm) and a quantum yield higher than 0.4. Dispersions of the selected fluorophore in poly(methyl methacrylate) (PMMA) thin films mostly maintained the optical features in solution with significant light transmittance in the visible region (90 % at 440 nm), and a brilliant green emission at about 500 nm. Photocurrent experiments performed on PMMA thin films coated over high purity transparent glasses foster their use in the realization of colourless luminescent solar concentrators with optical efficiencies close to 6 and useful for practical applications.

Keywords

push-pull imidazole-benzothiazole fluorophores, near-UV absorption, poly(methyl methacrylate), dye dispersion, luminescent solar concentrators

1. Introduction

Sunlight concentration is a promising path to cost-effective photovoltaic (PV) technologies. Compared to standard concentrators based on geometrical optics, luminescent solar concentrators (LSCs) show several advantages: low weight, high theoretical concentration factors, ability to work well with diffuse light and no needs of sun tracking or cooling apparatuses. LSCs are made of commodity materials with small amounts of a fluorescent component, and represent an extremely viable option for PV cells. Nowadays, the use of PV devices based on LSC technology has received a great impulse thanks to the modern building architectures that have inspired the photovoltaic application of colourful windows and panels. [1-3] LSCs consist in a slab of transparent material doped with a fluorophore able to absorb the solar spectrum.[4] The higher refractive index of the host compared to the environment makes it possible to trap a fraction of the emitted photons by means of total internal reflection. Photons are then collected at the edges of the device to produce electric power by means of photovoltaic (PV) cells. Moreover, the use of commodity plastics such as poly(methyl methacrylate) (PMMA) and polycarbonate (PC) and well consolidated and economic industrial processes for the preparation of LSCs offer encouraging means to include solar energy to the built environment.

However, conventional LSCs are often plagued by a multitude of unfavorable processes that hinder their ability to deliver light to PV cells, in particular fluorescence quenching due to aggregation phenomena between luminescent species.[4, 5] In the recent years, the research on PV devices based on LSC technology has been focusing on obtaining high power conversion efficiencies.[6-16] A simple approach for higher concentrations is to enhance the spectral window of absorption of the LSC, therefore increasing the number of available photons. To this end, multiple dye systems have long been proposed to cope for the narrow absorption characteristic of organic dyes as well as new design solutions.[12, 17, 18] Sloff et al.[16] described a stacked device with a power conversion efficiency of 7.1%, which is, at best of our knowledge, the highest efficiency ever reported for LSC-PV systems. Conversely, a dye mixture in a single slab offers the possibility of cascading of

emission via non-radiative processes such as the fluorescence resonance energy transfer (FRET).[17, 19] Nevertheless, the maximum efficiencies for LSCs were recorded for PMMAs device embedding perylene-based fluorophores[6, 8, 20]. Lumogen F Red 305 is a red-emitting perylene fluorophore, which is considered the state-of-the-art in dyes for LSC applications[4] since it shows a quantum yield (QY) of about 1 even at high concentration (>300 ppm) in polymers and in the solid state[21] and a good photostability.[22] However, its recent quotation at 7,500 €/kg by BASF might definitely affects the final cost of LSCs technology, thus limiting their worldwide distribution. Another disadvantage of typical LSC is the strong chromophore absorption in the visible spectrum, which leads to a large degree of colored tinting. In order to overcome this issue, visible-transparent LSCs based on NIR-emissive cyanine salts have been recently proposed as innovative devices with transparency of near 90% in the visible spectrum.[10] Although this technology is considered very promising, efforts are still required to translate discoveries into practical applications.

Herein, we exploited the potentiality offered by the new 1,4-phenylene-spaced azoles as near-UV absorbing fluorophores characterized by large Stokes shifts (SS) and green emission to be used in colorless LSC with optical efficiencies close to 6. Mixed imidazole-benzimidazole analogues were already proposed by us as fluorophores with SS near 100 nm, very high **Φ**, and with a bright blue-green emission well retained in the solid state. Notwithstanding their excellent emission features, their fluorescence peaked at $\lambda < 430$ nm does not match the working window of a Si-based PV cell ($\lambda \geq 500$ nm),[23] thus impeding their application in LSC technology.[24] Therefore, new push-pull imidazole-benzothiazole and thiazole-benzothiazole fluorophores, **1a-f** and **2a-c**, were efficiently synthesized in order to retain the features provided by the imidazole-benzimidazole analogues (**3a-c**) while shifting their emission to longer wavelengths.

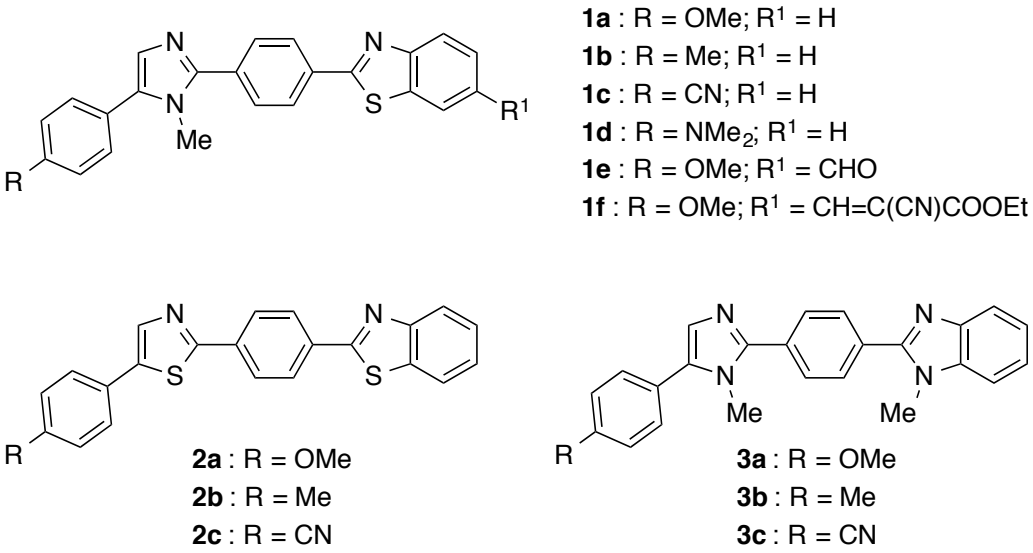

Figure 1. Chemical structure of compounds **1a-f**, **2a-c**, and **3a-c**

Thin-film LSC devices were then prepared by the dispersion of the best performing fluorophore in poly(methyl methacrylate) (PMMA) films coated over high optical quality glass slab. The LSC optical efficiencies were discussed and compared to that measured for LSC devices with the same geometry and containing Lumogen F Red 350.

2. Experimental part

2.1 Materials

Unless otherwise stated, all reactions were performed under argon by standard syringe, cannula and septa techniques. 2-(4-(5-(4-Methoxyphenyl)-1-methyl-1*H*-imidazol-2-yl)phenyl)-1-methyl-1*H*-benzo[d]imidazole (**3a**), 1-methyl-2-(4-(1-methyl-5-(*p*-tolyl)-1*H*-imidazol-2-yl)phenyl)-1*H*-benzo[d]imidazole (**3b**), 4-(1-methyl-2-(4-(1-methyl-1*H*-benzo[d]imidazol-2-yl)phenyl)-1*H*-imidazol-5-yl)benzonitrile (**3c**), and 2-(4-bromophenyl)-1-methyl-1*H*-benzo[*d*]imidazole (**6**) were prepared as previously described by us.[24] All the other commercially available reagents and solvents were used as received. Poly(methyl methacrylate) (PMMA, Aldrich, *Mw* = 350,000 g/mol, acid number <1 mg KOH/g).

*2.2 General procedures for the Palladium-catalyzed direct 5-arylation of 1-methyl-1H-imidazole (**8**) and thiazole (**9**) with aryl bromides **10a-c**.*[24, 25]

$Pd(OAc)_2$ (11.2 mg, 0.05 mmol), Bu_4NOAc (0.60 g, 2.0 mmol), and aryl bromide **10** (1.5 mmol), if a solid, were placed in a flame-dried reaction vessel. The reaction vessel was fitted with a silicon septum, evacuated, and back-filled with argon. This sequence was repeated twice more. DMA (5 mL), aryl bromide **10** (1.5 mmol), if a liquid, and the appropriate azole **8** or **9** (1.0 mmol) were then added successively under a stream of argon by syringe at room temperature. The resulting mixture was stirred under argon for 24h at 70 °C when thiazole (**9**) was employed, or at 110 °C when 1-methyl-1*H*-imidazole (**8**) was the coupling partner. After cooling to room temperature, the reaction mixture was diluted with AcOEt, filtered through a plug of Celite and eluted with additional AcOEt and CH_2Cl_2. The filtrate was concentrated under reduced pressure and the residue purified by flash chromatography on silica gel. This procedure was used to prepare compounds **4a-c** and **5a-c**.

*2.2.1 5-(4-Methoxyphenyl)-1-methyl-1H-imidazole (**4a**)*

The crude reaction product, which was obtained by Pd-catalyzed reaction of 1-methyl-1*H*-imidazole (**8**) with 4-bromoanisole (**10a**), was purified by flash chromatography on silica gel with a mixture of CH_2Cl_2 and MeOH (96:4) as eluent to give **4a** (0.15 g, 82 %) as a light-yellow solid,

m.p. 106-108 °C. ^{1}H NMR (200 MHz, $CDCl_3$): δ 7.48 (s, 1H), 7.30 (m, 2H), 7.02 (s, 1H), 6.96 (m, 2H), 3.83 (s, 3H), 3.61 (s, 3H) ppm. ^{13}C NMR (50.3 MHz, $CDCl_3$): δ 159.1, 138.3, 132.3, 129.6 (2C), 127.1, 121.8, 113.9 (2C), 55.1, 32.1 ppm. MS (EI): m/z (%) = 189 (12), 188 (100), 174 (10), 173 (82), 145 (17). The spectral properties of this compound are in agreement with those previously reported.[26]

*2.2.2 1-Methyl-5-(p-tolyl)-1H-imidazole (**4b**)*

The crude reaction product, which was obtained by Pd-catalyzed reaction of 1-methyl-1*H*-imidazole (**8**) with 4-bromotoluene (**10b**), was purified by flash chromatography on silica gel with a mixture of CH_2Cl_2 and MeOH (96:4) as eluent to give **4b** (0.14 g, 81 %) as a yellow oil. ^{1}H NMR (200 MHz, $CDCl_3$): δ 7.49 (s, 1H), 7.26 (m, 2H), 7.25 (m, 2H), 7.07 (s, 1H), 3.63 (s, 3H), 2.39 (s, 3H) ppm. ^{13}C NMR (50.3 MHz, $CDCl_3$): δ 138.7, 137.6, 133.3, 129.3 (2C), 128.3 (2C), 127.6, 126.7, 32.4, 21.2 ppm. MS (EI): m/z (%) = 173 (13), 172 (100), 171 (17), 144 (14), 130 (16). The spectral properties of this compound are in agreement with those previously reported.[27]

*2.2.3 4-(1-Methyl-1H-imidazol-5-yl)benzonitrile (**4c**)*

The crude reaction product, which was obtained by Pd-catalyzed reaction of of 1-methyl-1*H*-imidazole (**8**) with 4-bromobenzonitrile (**10c**), was purified by flash chromatography on silica gel with a mixture of CH_2Cl_2 and MeOH (96:4) as eluent to give **4c** (0.13 g, 69 %) as a light-yellow solid, m.p. 148-151 °C. 1H NMR (200 MHz, CDCl3): δ 7.73 (m, 2H), 7.59 (s, 1H), 7.53 (m, 2H), 7.22 (s, 1H), 3.75 (s, 3H) ppm. ^{13}C NMR (50.3 MHz, CDCl3): δ 140.5, 134.3, 132.5 (2C), 131.6, 129.8, 128.3 (2C), 118.5, 111.2, 33.0 ppm. MS (EI): m/z (%) = 159 (12), 158 (100), 130 (16), 116 (13), 103 (13), 89 (12). The spectral properties of this compound are in agreement with those previously reported.[25]

*2.2.4 5-(4-Methoxyphenyl)thiazole (**5a**)*

The crude reaction product, which was obtained by Pd-catalyzed reaction of thiazole (**9**) with 4-bromoanisole (**10a**), was purified by flash chromatography on silica gel with a mixture of toluene and AcOEt (92:8) as eluent to give **5a** (0.13 g, 67 %) as a bright-yellow solid, m.p. 89-92 °C. ^{1}H

NMR (200 MHz, $CDCl_3$): δ 8.68 (s, 1H), 7.97 (s, 1H), 7.48 (m, 2H), 6.92 (m, 2H), 3.82 (s, 3H) ppm. ^{13}C NMR (50.3 MHz, $CDCl_3$): δ 159.8, 151.2, 139.2, 138.0, 128.2 (2C), 123.6, 114.5 (2C), 55.4 ppm. MS (EI): m/z (%) = 191 (100), 176 (58), 149 (20), 148 (27), 121 (20). The spectral properties of this compound are in agreement with those previously reported.[28]

*2.2.5 5-(p-Tolyl)thiazole (**5b**)*

The crude reaction product, which was obtained Pd-catalyzed reaction of thiazole (**9**) with 4-bromotoluene (**10b**), was purified by flash chromatography on silica gel with a mixture of toluene and AcOEt (90:10 + 0.1 % Et_3N) as eluent to give **5b** (0.11 g, 65 %) as a pale-yellow solid, m.p. 82-84 °C. ^1H NMR (200 MHz, $CDCl_3$): δ 8.69 (s, 1H), 8.02 (s, 1H), 7.44 (m, 2H), 7.18 (m, 2H), 2.35 (s, 3H) ppm. ^{13}C NMR (50.3 MHz, $CDCl_3$): δ 151.4, 139.3, 138.4, 138.3, 129.6 (2C), 128.1, 126.7 (2C), 21.2 ppm. MS (EI): m/z (%) = 176 (12), 175 (100), 148 (32), 147 (43), 115 (17). The spectral properties of this compound are in agreement with those previously reported.[29]

*2.2.6 4-(Thiazol-5-yl)benzonitrile (**5c**)*

The crude reaction product, which was obtained by Pd-catalyzed reaction of thiazole (**9**) with 4-bromobenzonitrile (**10c**), was purified by flash chromatography on silica gel with a mixture of toluene and AcOEt (90:10) as eluent to give **5c** (0.11 g, 61 %) as a yellow solid, m.p. 101-102 °C. ^1H NMR (200 MHz, $CDCl_3$): δ 8.86 (s, 1H), 8.19 (s, 1H), 7.70 (m, 4H) ppm. ^{13}C NMR (50.3 MHz, $CDCl_3$): δ 153.7, 140.5, 137.2, 132.7, 135.3, 127.1, 118.2, 111.6 ppm. MS (EI): m/z (%) = 187 (%), 186 (100), 160 (10), 115 (10), 114 (12). The spectral properties of this compound are in agreement with those previously reported.[30]

*2.3 N,N-Dimethyl-4-(1-methyl-1H-imidazol-5-yl)aniline (**4d**)*

$Pd(OAc)_2$ (11.2 mg, 0.05 mmol), $P(2\text{-furyl})_3$ (23.2 mg, 0.1 mmol), K_2CO_3 (0.28 g, 2.0 mmol), and 4-bromo-*N.N*-dimethylanyline **10d** (0.30 g, 1.5 mmol) were placed in a flame-dried reaction vessel. The reaction vessel was fitted with a silicon septum, evacuated and back-filled with argon. This sequence was repeated twice more. DMA (5 mL) and 1-methyl-1*H*-imidazole (**8**) (80 μL, 82.1 mg, 1.0 mmol) were then added successively under a stream of argon by syringe at room temperature.

The resulting mixture was stirred at 110 °C under argon for 48h. After cooling to room temperature, the reaction mixture was diluted with EtOAc, filtered through a plug of Celite, and eluted with additional EtOAc and CH_2Cl_2. The filtrate was concentrated under reduced pressure, and the crude product was purified by flash chromatography on silica gel with a mixture of CH_2Cl_2 and MeOH (95:5) as eluent to give **4d** (0.15 g, 76 %) as a brown crystalline solid, m.p. 133-137 °C. ^{1}H NMR (400 MHz, $CDCl_3$): δ 7.49 (s, 1H), 7.28 (m, 2H), 7.02 (s, 1H), 6.79 (m, 2H), 3.65 (s, 3H), 3.02 (s, 6H) ppm. ^{13}C NMR (50.3 MHz, $CDCl_3$): δ 150.1, 137.6, 134.0, 129.5 (2C), 124.9, 116.3, 112.1 (2C), 40.3 (2C), 32.6 ppm. MS (EI): m/z (%) = 202 (14), 201 (100), 200 (42), 186 (13), 185 (17). Elemental analysis calcd (%) for $C_{12}H_{15}N_3$: C 71.61, H 7.51; found: C 71.68, H 7.49.

*2.4 2-(4-Bromophenyl)benzo[d]thiazole (**7a**)*[31, 32]

A three-necked 500 mL flask equipped with air condenser and magnetic stirrer was charged with 2-aminothiophenol (0.67 mL, 0.78 g, 6.25 mmol), 4-bromobenzaldehyde (0.93 g, 5 mmol) and DMSO (150 mL). The mixture was stirred under air at 190 °C. The progress of the reaction was monitored by GLC and after 2 h the conversion was found complete. The reaction mixture was poured into water and the resulting white-greenish precipitate was recovered by filtration, purified by crystallization in ethanol giving **7a** as a white solid (1.34 g, 92 %), m.p. 51-53 °C. ^{1}H NMR (200 MHz, $CDCl_3$): δ 8.09-8.05 (m, 1H), 8.00-7.89 (m, 3H), 7.66-7.60 (m, 2H), 7.51 (dt, J^1 = 8 Hz, J^2 = 1.4 Hz, 1H), 7.40 (dt, J^1 = 8 Hz, J^2 = 1.4 Hz, 1H) ppm. MS (EI): m/z (%) = 291 (100), 290 (20), 289 (99), 210 (30), 108 (19). The spectral properties of this compound are in agreement with those previously reported.[32]

*2.5 2-(4-Bromophenyl)-6-methylbenzo[d]thiazole (**7b**)*[33, 34]

According to a reported procedure,[33] in a three-necked 500 mL flask equipped with mechanic stirrer and dropping funnel were added 125 mL of glacial acetic acid that were cooled at 5 °C. A mixture of KSCN (5.83 g, 60 mmol) and *p*-toluidine (6.43 g, 60 mmol) was added to the precooled acetic acid giving a brownish solution. Then, a bromine solution (60 mmol of Br_2 in 60 mL glacial acetic acid) was added very slowly with constant stirring so that temperature did not rise above 5

°C. The reaction mixture was still stirred for additional 3 h. The hydrobromide salt obtained was filtered, the solid was dissolved in 150 mL of hot water and filtered once more. The solution was neutralized with ammonia and white crystals formed of 6-methylbenzo[*d*]thiazol-2-amine were collected. Afterwards, the intermediate obtained was refluxed with an aqueous solution of NaOH (5 times by weight of benzothiazole) until its own complete depletion. The solution was filtered and neutralized with glacial acetic acid. The separated yellowish semisolid formed was extracted with diethyl ether and dried over Na_2SO_4. The evaporation of the solvent and crystallization from MeOH/H_2O afforded 2,2'-disulfanediyilbis(4-methylaniline) as yellowish needle-shaped crystals (3.92 g, 47 %), m.p. 84-85 °C. ^{1}H NMR (400, $CDCl_3$): δ 6.98-6.95 (m, 4H), 6.64 (d, 2H, J = 8 Hz), 4.18 (bs, 4H, NH_2), 2.13 (s, 6H, CH_3) ppm. ^{13}C NMR (100 MHz): δ 146.3, 137.14, 132.4, 127.6, 119.0, 115.4, 20.1 ppm. MS (EI): m/z (%) = 277 (8), 276 (48), 139 (24), 138 (100), 94 (24), 77 (8).

2,2'-Disulfanediyilbis(4-methylaniline) (3.59 g, 13 mmol), bromobenzaldehyde (4.88 g, 26.4 mmol) and sodium metabisulfite (2.52 g, 13.26 mmol) were dissolved in DMSO (100 mL). The resulting orange reaction mixture was stirred at 120 °C and the formation of the desired product monitored by TLC and GC analyses. After 4 h, the reaction mixture was cooled at room temperature, water was added (200 mL) and the resulting precipitate was collected by vacuum filtration. Afterwards, the solid was well washed with excess water (150 mL) in order to remove residual DMSO, re-dissolved in CH_2Cl_2 and finally washed with brine. The organic layer was dried over Na_2SO_4 and the solvent removed *in vacuo* giving compound **7b** as a yellow solid (5.14 g, 64 %), m.p. 175-178 °C. ^{1}H NMR (400, $CDCl_3$): δ 7.95-7.93 (m, 3H), 7.69 (s, 1H), 7.62 (d, 2H, J = 8 Hz), 7.31 (dd, 1H, J^1 = 8 Hz, J^2 = 2 Hz), 2.50 (s, 3H) ppm. ^{13}C NMR (100 MHz, $CDCl_3$) 165.6, 152.2, 135.6, 135.2, 132.7, 132.2, 129.1, 128.2, 125.1, 123.3, 121.4, 21.6 ppm. MS (EI): m/z (%) = 306 (17), 305 (100), 304 (36), 303 (95), 302 (21). The spectral properties of this compound are in agreement with those previously reported.[34]

2.6 2-(4-Bromophenyl)benzo[d]thiazole-6-carbaldehyde ***(7c)***

A two-necked 1 L flask equipped with condenser was charged with 2-(4-bromophenyl)-6-methylbenzo[*d*]thiazole (**7b**) (5 g, 16.4 mmol), *N*-bromosuccinimide (6.12 g, 34.4 mmol) and AIBN (0.43 g, 2.6 mmol). The reaction vessel was fitted with a silicon septum, then evacuated and back-filled with argon for three times. After that, degassed benzene (320 mL) was added and the reaction mixture was left to reflux 6 h. The reaction was filtered and the solvent was removed *in vacuo*. The solid obtained was dissolved in CH_2Cl_2, washed with water (3 times) and brine, thus dried over Na_2SO_4. The crude product was a mixture of monobrominated and dibrominated compound (30:70, respectively) as shown by ^{1}H NMR. The mixture of brominated products obtained (7.52 g) was added without further purification to a two-necked 500 mL flask equipped with a condenser and magnetic stirrer. The reaction vessel was evacuated and back-filled with argon for three times. $AgNO_3$ (6.27 g, 36.9 mmol) and 200 mL anhydrous 1,2-dimethoxyethane were then added and the reaction mixture was allowed to reflux until the complete disappearance of the precursor. Anhydrous triethylamine (23 mL, 164 mmol) was finally added and the reaction was refluxed 2 h more. Afterwards, CH_2Cl_2 was poured to the reaction mixture that was filtered on a layer of Celite. The solvent was removed and the crude product was dissolved again in CH_2Cl_2, washed with water (3 times) and brine and dried over Na_2SO_4. The solid obtained after evaporation of the solvent was recrystallized from CH_2Cl_2/hexane giving product **7c** as an off-white solid (3.28 g, 63 %), m.p. 305-309 °C. ^{1}H NMR (400, $CDCl_3$): δ 10.12 (s, 1H, CHO), 8.45 (d, 1H, J = 2 Hz), 8.17 (d, 1H, J = 8 Hz), 8.03 (dd, 1H, J^1 = 8 Hz, J^2 = 2 MHz), 7.99 (m, 2H), 7.67 (m, 2H) ppm. ^{13}C NMR (100 MHz, $CDCl_3$): δ 191.1, 171.3, 158.1, 135.8, 133.6, 132.6 (2C), 132.1, 129.3 (2C), 127.6, 126.6, 124.5, 123.9 ppm. MS (EI): m/z (%) = 319 (100), 318 (79), 317 (94), 316 (64), 209 (32). Elemental analysis calcd (%) for $C_{14}H_8BrNOS$: C 52.85, H 2.53; found: C 52.89, H 2.52.

*2.7 General procedures for the Pd-catalyzed C-2 arylation of 5-aryl-imidazoles (**4a-d**) and 5-aryl-thiazoles (**5a-c**) with bromides **7a** and **7c***

Method A:[35-37]

A two-necked flask equipped with a magnetic stirrer and a reflux condenser was charged with the

appropriate 5-aryl-1-methyl-1*H*-imidazole **4a-c** (1 mmol) or 5-aryl-thiazoles **5a-c** (1 mmol), 2-(4-bromophenyl)benzo[*d*]thiazole (**7a**) (1.1 mmol), $Pd(OAc)_2$ (11.2 mg, 0.05 mmol) and CuI (381 mg, 2 mmol). The apparatus was fitted with a silicon septum, evacuated and back-filled with argon three times. Anhydrous DMA (5 mL) was added by syringe against a positive pressure of argon. The reaction mixture was stirred at 160 °C. The reaction evolution was followed by GLC and GLC-MS analyses. After cooling at room temperature, the reaction mixture was diluted with CH_2Cl_2 (200 mL) and poured into a saturated aqueous NH_4Cl solution to which 5 mL of concentrated aqueous ammonia had been added. The resulting mixture was stirred in the open air for 30 minutes and then extracted with CH_2Cl_2. The organic extracts were washed with saturated brine, dried, concentrated under reduced pressure, and the resulting crude reaction product was purified as described below. This procedure was used to prepare compounds **1a**, **1b**, **1c**, **2a**, **2b**, and **2c**.

Method B:[25]

A two-necked flask equipped with a magnetic stirrer and a reflux condenser was charged with the 5-aryl-1-methyl-1*H*-imidazole **4a**, or **4d** (1 mmol), 2-(4-bromophenyl)benzo[*d*]thiazole (**7a**) or 2-(4-bromophenyl)benzo[*d*]thiazole-6-carbaldehyde (**7c**) (1.1 mmol), $Pd(OAc)_2$ (11.2 mg, 0.05 mmol), Bu_4NOAc (0.60 g, 2 mmol) and CuI (380.9 mg, 2 mmol). The apparatus was fitted with a silicon septum, evacuated and back-filled with argon three times. Anhydrous DMA (5 mL) was added by syringe against a positive pressure of argon. The reaction mixture was stirred at 110 °C for 24 h. The reaction evolution was followed by TLC analysis. After cooling at room temperature, the reaction mixture was diluted with CH_2Cl_2 (100 mL) and poured into a saturated aqueous NH_4Cl solution to which 5 mL of concentrated aqueous ammonia had been added. The resulting mixture was stirred in the open air for 30 minutes and the organic layer was extracted. The solvent was removed and the solid crude product was well washed with water in order to remove the excess of Bu_4NOAc, filtered, re-dissolved in CH_2Cl_2, washed with saturated brine, dried and concentrated under reduced pressure. The resulting crude reaction product was purified by crystallization. This procedure was used to prepare compounds **1d** and **1e**.

*2.7.1 2-(4-(5-(4-Methoxyphenyl)-1-methyl-1H-imidazol-2-yl)phenyl)benzo[d]thiazole (**1a**).*

The crude reaction product obtained by Pd- and Cu-mediated reaction of **4a** and **7a** according to *Method A* was purified by treatment with a hot mixture of toluene and AcOEt (70:30), followed by filtration. The solid recovered (0.09g) resulted to be pure **1a**, while the filtrate was further purified by flash chromatography on silica gel using a mixture of toluene and AcOEt (70:30) as eluent. The chromatographic fractions containing the product were collected, concentrated and added to the solid previously recovered by filtration. In this way pure **1a** was obtained as a yellow solid (0,14 g, 66 %), m.p. 244-248 °C. ^{1}H NMR (200 MHz, $CDCl_3$): δ 8.21 (m, 2H), 8.10 (d, J = 8.0 Hz, 1H), 7.93 (d, J = 8.0 Hz, 1H), 7.86 (m, 2H), 7.55-7.37 (m, 4H), 7.20 (s, 1H), 7.01 (m, 2H), 3.87 (s, 3H), 3.71 (s, 3H) ppm. ^{13}C NMR (50.3 MHz, $CDCl_3$): δ 167.2, 159.5, 154.1, 147.9, 135.9, 135.1, 133.4, 133.3, 130.2, 129.0, 127.7, 127.5, 126.4, 125.3, 123.3, 122.3, 121.7, 114.3, 55.4, 34.0 ppm. MS (EI): m/z (%) = 398 (30), 397 (100), 396 (27), 382 (15), 198 (13). Elemental analysis calcd (%) for $C_{24}H_{19}N_3OS$: C 72.52, H 4.82; found: C 72.49, H 4.80.

*2.7.2 2-(4-(1-Methyl-5-(p-tolyl)-1H-imidazol-2-yl)phenyl)benzo[d]thiazole (**1b**)*

The crude reaction product obtained by Pd- and Cu-mediated reaction of **4b** and **7a** according to *Method A* was purified by flash chromatography on silica gel with a mixture of toluene and AcOEt (60:40) as eluent to give **1b** as an iridescent yellow-greenish solid (0.12 mg, 66 %), m.p. 204-206 °C. ^{1}H NMR (200 MHz, $CDCl_3$): δ 8.21 (m, 2H), 8.10 (dd, J^1 = 8.0 Hz, J^2 = 0.6 Hz, 1H), 7.93 (m, 1H), 7.86 (m, 2H), 7.56-7.23 (m, 8H), 3.74 (s, 3H), 2.42 (s, 3H) ppm. ^{13}C NMR (50.3 MHz, $CDCl_3$): δ 167.2, 154.1, 148.1, 138.0, 136.2, 135.1, 133.4, 133.2, 129.5, 129.0, 128.8, 128.6, 127.7, 127.0, 126.4, 125.3. 123.3, 121.6, 34.0, 21.3 ppm. MS (EI): m/z (%) = 383 (9), 382 (30), 381 (100), 380 (49), 190 (14). Elemental analysis calcd (%) for $C_{24}H_{19}N_3S$: C 75.56, H 5.02; found: C 75.59, H 5.03.

*2.7.3 4-(2-(4-(Benzo[d]thiazol-2-yl)phenyl)-1-methyl-1H-imidazol-5- yl)benzonitrile (**1c**)*

The crude reaction product obtained by Pd- and Cu-mediated reaction of **4c** and **7a** according to *Method A* was purified by flash chromatography on silica gel with a mixture of toluene and AcOEt

(40:60) as eluent to give **1c** as a yellow solid (0.15 g, 83 %), m.p. 217-220 °C. ^{1}H NMR (200 MHz, $CDCl_3$): δ 8.24 (m, 2H), 8.11 (d, *J* = 7.4 Hz, 1H), 7.94 (d, *J* = 8.4 Hz, 1H), 7.86 (m, 2H), 7.77 (m, 2H), 7.60 (m, 2H), 7.53-7.37 (m, 3H), 3.78 (s, 3H) ppm. ^{13}C NMR (50.3 Hz, $CDCl_3$): δ 166.9, 154.1, 150.0, 135.1, 134.4, 134.3, 134.0, 132.7, 132.4, 129.7, 129.3, 128.5, 127.8, 126.5, 125.5, 123.4, 121.7, 118.5, 111.4, 34.4 ppm. MS (EI): m/z (%) = 394 (9), 393 (27), 392 (100), 391 (66), 196 (10). Elemental analysis calcd (%) for $C_{24}H_{16}N_4S$: C 73.45, H 4.11; found: C 73.50, H 4.09.

*2.7.4 4-(2-(4-(Benzo[d]thiazole-2-yl)phenyl)-1-methyl-1H-imidazol-5-yl)-N,N-dimethylaniline (**1d**)*

The crude reaction product obtained by Pd- and Cu-mediated reaction of **4d** and **7a** according to *Method B* was purified by crystallization from toluene to give **1d** as a yellow solid (0.19 g, 46 %), m.p. 220-225 °C. ^{1}H NMR (400 MHz, $CDCl_3$): δ 8.19 (m, 2H), 8.09 (d, *J* = 8 Hz, 1H), 7.92 (d, *J* = 8 Hz, 1H), 7.86 (m, 2H), 7.51 (t, *J* = 8 Hz, 1H), 7.40 (t, *J* = 8 Hz, 1H), 7.33 (m, 2H), 7.16 (s, 1H), 6.80 (m, 2H), 3.71 (s, 3H), 3.01 (s, 6H) ppm. ^{13}C NMR (50.3 MHz, $CDCl_3$): δ 167.5, 154.3, 150.3, 147.7, 137.0, 135.2, 133.7, 133.3, 129.9, 129.0, 127.8, 127.1, 126.5, 125.4, 123.4, 122.4, 121.8, 117.6, 112.4, 40.5, 34.0 ppm. HRMS (ESI) m/z found $[M+H]^+$ 411.1645; $C_{25}H_{22}N_4S$ requires $[M+H]^+$ 411.1638.

*2.7.5 2-(4-(5-(4-Methoxyphenyl)-1-methyl-1H-imidazol-2-yl)phenyl)benzo[d]thiazole-6-carbaldehyde (**1e**)*

The crude reaction product obtained by Pd- and Cu-mediated reaction of **4a** and **7c** according to *Method B* was purified by crystallization from AcOEt to give **1e** as a yellow solid (0.44 g, 68 %), m.p. 254-257 °C. ^{1}H NMR (400 MHz, $CDCl_3$): δ 10.13 (s, 1H), 8.48 (d, *J* = 2 Hz, 1H), 8.25 (m, 2H), 8.20 (d, *J* = 8 Hz, 1H), 8.03 (dd, J^1 = 8 Hz, J^2 = 2 Hz, 1H), 7.90 (m, 2H), 7.40 (m, 2H), 7.20 (s, 1H), 7.01 (m, 2H), 3.88 (s, 3H), 3.73 (s, 3H) ppm. ^{13}C NMR (100 MHz, $CDCl_3$): 191.2, 171.9, 159.8, 158.2, 147.8, 136.3, 135.8, 134.3, 133.5, 132.9, 130.3, 129.2, 128.1, 127.8, 127.6, 124.6, 123.9, 114.5, 55.5, 34.1 ppm. HRMS (ESI) m/z found $[M+H]^+$ 426.1276; $C_{25}H_{19}N_3O_2S$ requires $[M+H]^+$ 426.1271.

*2.7.6 2-(4-(5-(4-Methoxyphenyl)thiazol-2-yl)phenyl)benzo[d]thiazole (**2a**)*

The crude reaction product obtained by Pd- and Cu-mediated reaction of **5a** and **7a** according to *Method A* was treated with hot AcOEt and filtered. The solid recovered by filtration was further treated with hot CH_2Cl_2, filtered and concentrated. In this way a first aliquot of **2a** was recovered (26 mg). The solution obtained from the first filtration was purified by flash chromatography on silica gel with a mixture of CH_2Cl_2 and AcOEt (96:4) as eluent. The chromatographic fractions containing the product were collected, concentrated and added to the first aliquot of **2a**, to give the required product as an iridescent yellow solid (0.14 g, 72 %), m.p. 196-199 °C. ^{1}H NMR (200 MHz, $CDCl_3$): δ 8.20-8.05 (m, 5H), 7.97-7.91 (m, 2H), 7.58-7.37 (m, 4H), 6.96 (m, 2H), 3.86 (s, 3H) ppm. ^{13}C NMR (100 MHz, acquired at 40 °C, $CDCl_3$): δ 167.2, 165.1, 160.2, 154.5, 140.3, 138.9, 136.1, 135.4, 134.8, 128.3, 126.9, 126.6, 125.6, 124.1, 123.6, 121.8, 114.8, 55.6 ppm. MS (EI): m/z (%) = 400 (100), 281 (22), 207 (38), 149 (32), 44 (24). Elemental analysis calcd (%) for $C_{23}H_{16}N_2OS_2$: C 68.97, H 4.03; found: C 70.01, H 4.02.

*2.7.7 2-(4-(5-(p-Tolyl)thiazol-2-yl)phenyl)benzo[d]thiazole (**2b**)*

The crude reaction product obtained by Pd- and Cu-mediated reaction of **5b** and **7a** according to *Method A* was purified adding a mixture of toluene and AcOEt (95:5), filtrating an insoluble residual and performing a flash chromatography on silica gel of the filtrate to give **2b** as a yellow solid (47 mg, 25 %), m.p. 207-210 °C. ^{1}H NMR (200 MHz, $CDCl_3$): δ 8.21-8.16 (m, 2H), 8.12-8.06 (m, 3H), 8.03 (s, 1H), 7.93 (d, J = 8.0 Hz, 1H), 7.56-7.40 (m, 4H), 7.24 (m, 2H), 2.40 (s, 3H) ppm. ^{13}C NMR (100 MHz, $CDCl_3$): δ 167.2, 165.5, 154.4, 140.5, 139.3, 138.8, 136.0, 135.3, 134.8, 130.0, 128.5, 128.3, 126.9, 126.8, 126.7, 125.6, 123.5, 121.8, 21.4 ppm. MS (EI): m/z (%) = 385 (26), 384 (100), 192 (12), 148 (26), 147 (31). Elemental analysis calcd (%) for $C_{23}H_{16}N_2S_2$: C 71.84, H 4.19; found: C 71.78, H 4.20.

*2.7.8 4-(2-(4-(Benzo[d]thiazol-2-yl)phenyl)thiazol-5-yl)benzonitrile (**2c**)*

The crude reaction product obtained by Pd- and Cu-mediated reaction of **5c** and **7a** according to *Method A* was treated with boiling CH_2Cl_2 for 2h, filtered and concentrated, to give **2c** as a yellow solid (96 mg, 53 %), m.p. 233- 235 °C. ^{1}H NMR (200 MHz, acquired at 40 °C, $CDCl_3$): δ 8.23-8.08

(m, 6H), 7.93 (d, *J* = 7.6 Hz, 1H), 7.71 (s, 4H), 7.56-7.38 (m, 2H) ppm. ^{13}C NMR (100 MHz, acquired at 40 °C, $CDCl_3$): δ 168.0, 166.9, 154.4, 141.5, 138.0, 135.9, 135.7, 135.4, 133.13, 128.4, 127.3, 127.2, 126.7, 125.8, 123.7, 121.9, 118.5, 112.1 ppm. MS (EI): m/z (%) = 397 (12), 396 (29), 395 (100), 197 (8), 159 (52). Elemental analysis calcd (%) for $C_{23}H_{13}N_3S_2$: C 69.85, H 3.31; found: C 69.79, H 3.29.

*2.8 Ethyl 2-cyano-3-(2-(4-(5-(4-methoxyphenyl)-1-methyl-1H-imidazol)phenyl)benzo[d]thyazol-6-yl)acrylate (**1f**)*

According to a reported procedure,[38] a two-necked 10 mL flask equipped with a condenser was charged with compound **1e** (64 mg, 0.15 mmol) and imidazole (2 mg, 0.03 mmol). The reaction vessel was fitted with a silicon septum, then evacuated and back-filled with argon for three times. Then, dichloromethane (1 mL) and ethyl 2-cyanoacetate (16 μL, 0.15 mmol) were added and the reaction mixture was heated to reflux overnight. The yellow crude product was worked-up by diluting with CH_2Cl_2 and washing with water three times. The organic layer was dried over Na_2SO_4, the solvent was evaporated and the crude product was purified by washing with 5 mL of diethyl ether, giving compound **2f** as a yellow-orange solid (70 mg, 90%), m.p. 231-235 °C. ^{1}H-NMR (200 MHz, $CDCl_3$): 8.67 (d, *J* = 2 Hz, 1H), 8.36 (s, 1H), 8.24 (m, 2H), 8.16 (d, *J* = 8 Hz, 1H), 8.09 (dd, J^1 = 8 Hz, J^2 = 2 Hz, 1H), 7.89 (m, 2H), 7.40 (m, 2H), 7.20 (s, 1H), 7.02 (m, 2H), 4.42 (q, *J* = 8 Hz, 2H), 3.87 (s, 3H), 3.73 (s, 3H), 1.42 (t, *J* = 8 Hz, 3H) ppm. ^{13}C-NMR (100 MHz, $CDCl_3$): 171.8, 162.7, 159.9, 157.3, 154.3, 147.8, 136.4, 136.3, 134.4, 132.9, 130.4, 129.8, 129.3, 128.6, 128.2, 127.8, 124.9, 124.0, 122.4, 115.9, 114.5, 102.7, 63.0, 55.5, 34.1, 14.3 ppm. HRMS (ESI) m/z found $[M+H]^+$ 521.1646; $C_{30}H_{24}N_4O_3S$ requires $[M+H]^+$ 521.1642.

2.9 Preparation of polymer films for optical studies

Different fluorophore/PMMA thin films were prepared by drop casting, i.e. pouring 0.8 mL chloroform solution containing 30.5 mg of the polymer and the proper amount of fluorophore to obtain concentrations in the range 0.1–2.0 wt.% on 35x50 mm area over a glass surface. The glass

slides were cleaned with chloroform and immerged in 6 M HCl for at least 12 h, then they were rinsed with water, acetone and isopropanol and dried for 8 h at 120 °C. Solvent evaporation was performed on a warm hot plate (about 30 °C) and in a closed environment. The film thickness was measured by a Starrett micrometer to be 25±5 μm. The PMMA films were easily removed with a spatula after immersion in water so that they can be stored for successive measurements and comparison by attaching them on 50x50x3 mm optically pure glass substrate (Edmund Optics Ltd BOROFLOAT window 50x50 TS) with a high-purity silicone oil with a refractive index comparable to PMMA and glass (i.e., poly(methylphenyl siloxane), 710 fluid, Aldrich, refractive index n = 1.5365). Absorption and emission properties of such devices showed negligible differences with the freshly prepared ones.

2.10 Apparatus and Methods

Melting points were recorded on a hot-stage microscope (Reichert Thermovar). Fluka precoated silica gel PET foils were used for TLC analyses. GLC analyses were performed on a Dani GC 1000 instrument equipped with a PTV injector using two types of capillary columns: an Alltech AT-35 bonded FSOT column (30 m x 0.25 mm i.d.) and an Alltech AT-1 bonded FSOT column (30 m x 0.25mm i.d.). Purifications by flash chromatography were performed using silica gel Merck 60 (particle size 0.040-0.063 mm). EI-MS spectra were recorded at 70 eV by GLC-MS, performed on an Agilent 6890N gas-chromatograph interfaced with Agilent 5973N mass detector. NMR spectra were recorded at room temperature at 400 MHz (^{1}H) and 100 MHz (^{13}C), or 200 MHz (^{1}H) and 50.3 MHz (^{13}C) and were referred to TMS or to the residual protons of deuterated solvents.

ESI-Q/ToF flow injection analyses (FIA) were carried out using a 1200 Infinity HPLC (Agilent Technologies, USA), coupled to a Jet Stream ESI interface (Agilent) with a Quadrupole-Time of Flight tandem mass spectrometer 6530 Infinity Q-TOF (Agilent Technol- ogies). Two sets of eluents were used: 100% MeOH or 85% H_2O and 15% acetonitrile, both added with 1% formic acid. The flow rate was 0.2 mL/min. Injection volume: 3 mL. The ESI operating conditions were:

drying gas (N_2, purity >98%): 350° C and 10 L/min; capillary voltage 4.5 KV; nebuliser gas 35 psig; sheath gas (N_2, purity >98%): 375° C and 11 L/min.

Absorption spectra were recorded at room temperature on a Perkin-Elmer Lambda 650 spectrometer. Fluorescence spectra were measured at room temperature on a Horiba Jobin-Yvon Fluorolog®-3 spectrofluorometer and equipped with a 450 W xenon arc lamp, double-grating excitation and single-grating emission monochromators. The fluorescence of dye/PMMA films were recorded by using the Solid-Sample Holder and collecting the front-face emission at 30°.

The fluorescence quantum yield (Φ_f) in $CHCl_3$ was determined at room temperature relative to quinine sulphate ($\Phi^s_f = 0.54$ in 0.1 M H_2SO_4) using the following relation:[39]

$$\Phi_X = \Phi_{ST}\left(\frac{Grad_X}{Grad_{ST}}\right)\left(\frac{\eta_X^2}{\eta_{ST}^2}\right)$$

Where the subscripts ST and X are standard and dye respectively, Grad the gradient from the plot of integrated fluorescence intensity vs absorbance for different solutions of standard and dyes. In order to minimise re-absorption effects absorbances never exceed 0.1 at and above the excitation wavelength. η is the refractive index of the solvent, i.e. 1.45 for $CHCl_3$ and 1.333 for water.[40] The emission quantum yields of the solid films were obtained by means of a 152 mm diameter "Quanta-phi" integrating sphere coated with Spectralon® and mounted in the optical path of the spectrofluorimeter, using as an excitation source a 450 W Xenon lamp coupled with a double-grating monochromator for selecting wavelengths.

2.10 Photocurrent measurements

A proper apparatus was build and composed by a plywood wooden box 15x15x30 cm with walls 1.5 cm thick. A removable cover hosting a housing for a solar lamp is present at the top. During the measurement a solar lamp TRUE-LIGHT® ESl E27 20W was used. Two 50x3 mm slits were carved out at 5 cm from the bottom of the box to exactly fit the LSC systems (dimensions 50x50x3 mm) so that the minimum amount of light would come out during the measurement conditions. On the outer side of the slit, a set of three 1x1 cm photodiodes (THORLABS FDS1010 Si photodiode, with an active area of 9.7 x 9.7 mm and high responsivity (A/W) in the spectral range of 400–1100

nm) connected in parallel fashion was placed and coupled to a multimeter (KEITHLEY Mod. 2700) for photocurrent measuring. In order to collect a more intense and stable output signal, both the photodiodes and the multimeter are connected to an amplifier, realized in laboratory, following the specifications given by THORLABS. The measurement procedure comprehends a 20 minutes warm-up for the lamp, in order to reach its maximum power output. After this time, the current intensity can be measured every minute, for a total of five minutes.

2.11 Efficiency measurement using a PV-cell

A different set of LSC samples was prepared to measure the concentration efficiency attaching a Si-PV cell (IXYS SLMD121H08L mono solar cell 86x14 mm, with a solar cell efficiency of 22% and a fill factor > 70%) to one edge of the sample. This set of samples was made covering the full 50x50 area of the previously introduced optically pure glass slabs with a 24±5 μm dye/PMMA thick film. One edge of the LSC was connected to a Si–based PV cell masked to cover just the LSC edge (50x3 mm) using silicone grease while the remaining edges were covered with an aluminum tape. These devices where then placed over a white poly(ethylene terephthalate) scattering sheet (Microcellular® MCPET reflective sheet, ERGA TAPES Srl) and placed about 20 cm under a solar lamp (TRUELIGHT® ESL E27 20W, with a correlated color temperature of 5500 K). The efficiency is reported as η_{opt}, which is the ratio between the short circuit current of the PV cell attached the LSC edges under illumination of a light source (I_{LSC}) and the short circuit current of the bare cell put perpendicular to the light source (I_{SC}).

2. Results and discussion

3.1 Synthesis of mixed azole-benzazole-based dyes

Imidazole-benzothiazole-based dyes **1** and thiazole-benzothiazole analogues **2** were prepared according to the retrosynthetic pathway reported in Scheme 1. This approach resembles that adopted by us for the synthesis of the already reported imidazole-benzimidazole dyes **3.**[24]

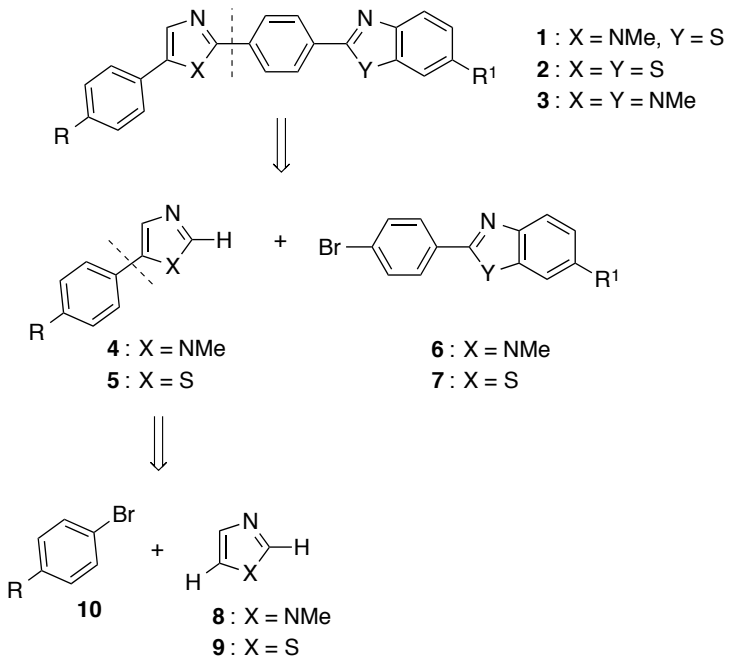

Scheme 1. Retrosynthetic pathway for compounds **1**, **2** and **3**

This two-step sequence involves at first a regioselective direct C5 arylation of 1-methyl-1*H*-imidazole (**8**) or thiazole (**9**) with aryl bromides **10a-d**. This coupling, catalyzed by $Pd(OAc)_2$ and promoted by Bu_4NOAc (1) or K_2CO_3,[36-38] allowed the preparation of the required 5-arylazoles **4a-d** and **5a-c** in 61-92% isolated yield (Scheme 2). Azoles **4a-c** and **5a-c** were then reacted with 2-(4-bromophenyl)-benzothiazole (**7a**) according to our protocol for the base-free and ligandless protocol for the direct C2 arylation of azoles,[35-37] mediate by Pd and Cu, in DMA at 160 °C for 72h (Method A, Scheme 2). In this way the required dyes **1a-c** and **2a-c** were isolated in 25-83% yield.

However, the base-free protocol proved to be unsuitable for the synthesis of compounds **1d** and **1e**, due to the high reaction temperature. With our delight, these two derivatives were successfully prepared using Bu_4NOAc as an additive, which allowed us to carry out the coupling at 110 °C instead of 160 °C, in DMA for 24h.[25] According to this procedure, **1d** and **1e** were obtained in 46 and 68% isolated yield, respectively, by Pd/Cu-mediated direct C2 arylation of 5-arylimidazoles **4d** and **4a** with bromobenzothiazoles **7a** and **7b** (Scheme 2). All the intermediates and products were characterized by NMR spectroscopy and mass spectrometry, with satisfactory results.

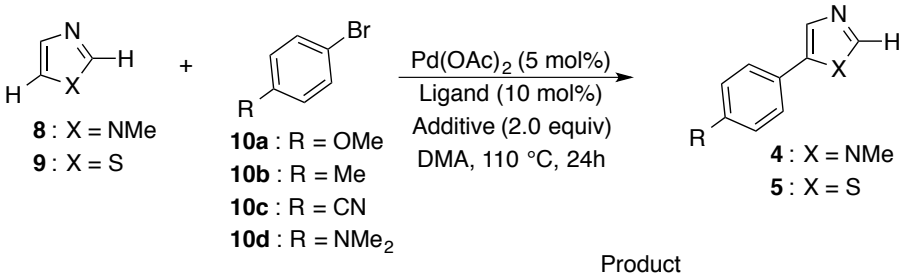

azole	10	Ligand	Additive	Product 4 or 5	R	Yield (%)
8	**a**	-	Bu_4NOAc	**4a**	OMe	82
8	**b**	-	Bu_4NOAc	**4b**	Me	81
8	**c**	-	Bu_4NOAc	**4c**	CN	69
8	**d**	P(2-furyl)$_3$	K_2CO_3	**4d**	NMe_2	76
9	**a**	-	Bu_4NOAc	**5a**	OMe	67
9	**b**	-	Bu_4NOAc	**5b**	Me	65
9	**c**	-	Bu_4NOAc	**5c**	CN	61

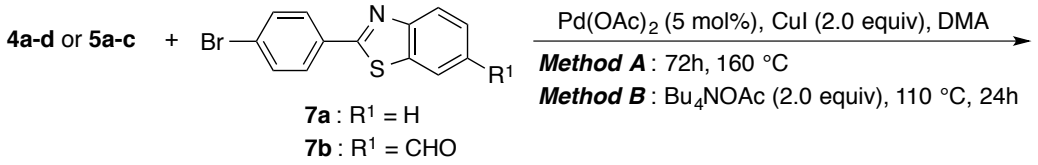

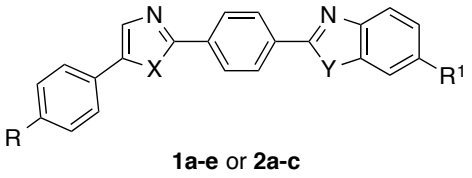

1 or 2	X	R	R^1	Method	Yield (%)
1a	NMe	OMe	H	A	66
1b	NMe	Me	H	A	66
1c	NMe	CN	H	A	83
1d	NMe	NMe_2	H	B	46
1e	NMe	OMe	CHO	B	68
2a	S	OMe	H	A	72
2b	S	Me	H	A	25
2c	S	CN	H	A	53

Scheme 2. Synthesis of compounds **4a-d**, **5a-c**, **2a-e** and **3a-c**

Finally, compound **1f** was obtained in 90 % isolated yield by Knoevenagel condensation of **1e** with ethyl cyanoacetate in CH_2Cl_2 (Scheme 3).[38]

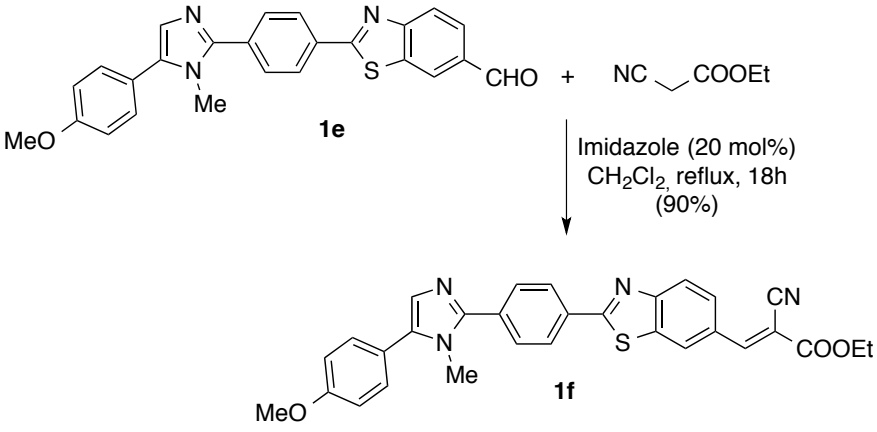

Scheme 3. Synthesis of compound **1f**

3.2 Optical properties in $CHCl_3$ solutions

All the optical features of compounds **1a-f** and **2a-c** are summarized in Table 1 and compared to that of imidazole-benzimidazole analogues (**3a-c**) recently published by our group.[24]

Table 1 Spectroscopic properties of fluorophores **1a-f**, **2a-c** and **3a-c** dissolved in $CHCl_3$

	λ_{abs} [nm]	ε [$M^{-1}cm^{-1}$]	λ_{em} [nm]	SS [nm]	Φ_f[a]
1a	345	32,000	457	112	0.90
1b	342	32,000	442	100	0.81
1c	343	42,000	426	83	0.80
1d	351	32,700	518	165	0.42
1e	363	19,000	506	143	0.50
1f	385	38,000	532	147	0.11
2a	372	38,800	460	88	0.61
2b	367	43,000	443	76	0.59
2c	372	47,500	436	64	0.55
3a	320	36,000	427	107	0.90
3b	316	31,000	416	100	0.88
3c	328	39,000	415	87	0.83

[a]Fluorescence quantum yield (Φ) was determined relative to quinine sulphate in 0.1M H_2SO_4 (Φ = 0.54).

The absorption features of the **1a** and **1b** imidazole-benzothiazole fluorophores are basically the same, with absorption bands peaked around 342-345 nm. **1c** absorbs in the same range but shows higher extinction coefficient as analogously reported for imidazole-benzoimidazole **3a-c** fluorophores.[24] This characteristic is also reflected in fluorescence since the emission spectrum becomes progressively red-shifted in the order **1c**, **1b**, **1a**, and the Stokes shift (SS) thus increases in the same direction (Figure 1). The fluorescence quantum yields (Φ) of the three fluorophores were also determined to have a quantitative picture (Table 1). All molecules resulted strong emitters with quantum yields comprised between 0.8 and 0.9. The lowest Φ corresponds to **1c** that shows the lowest SS (83 nm) due to the highest overlapping between absorbance and emission (Figure 1a).

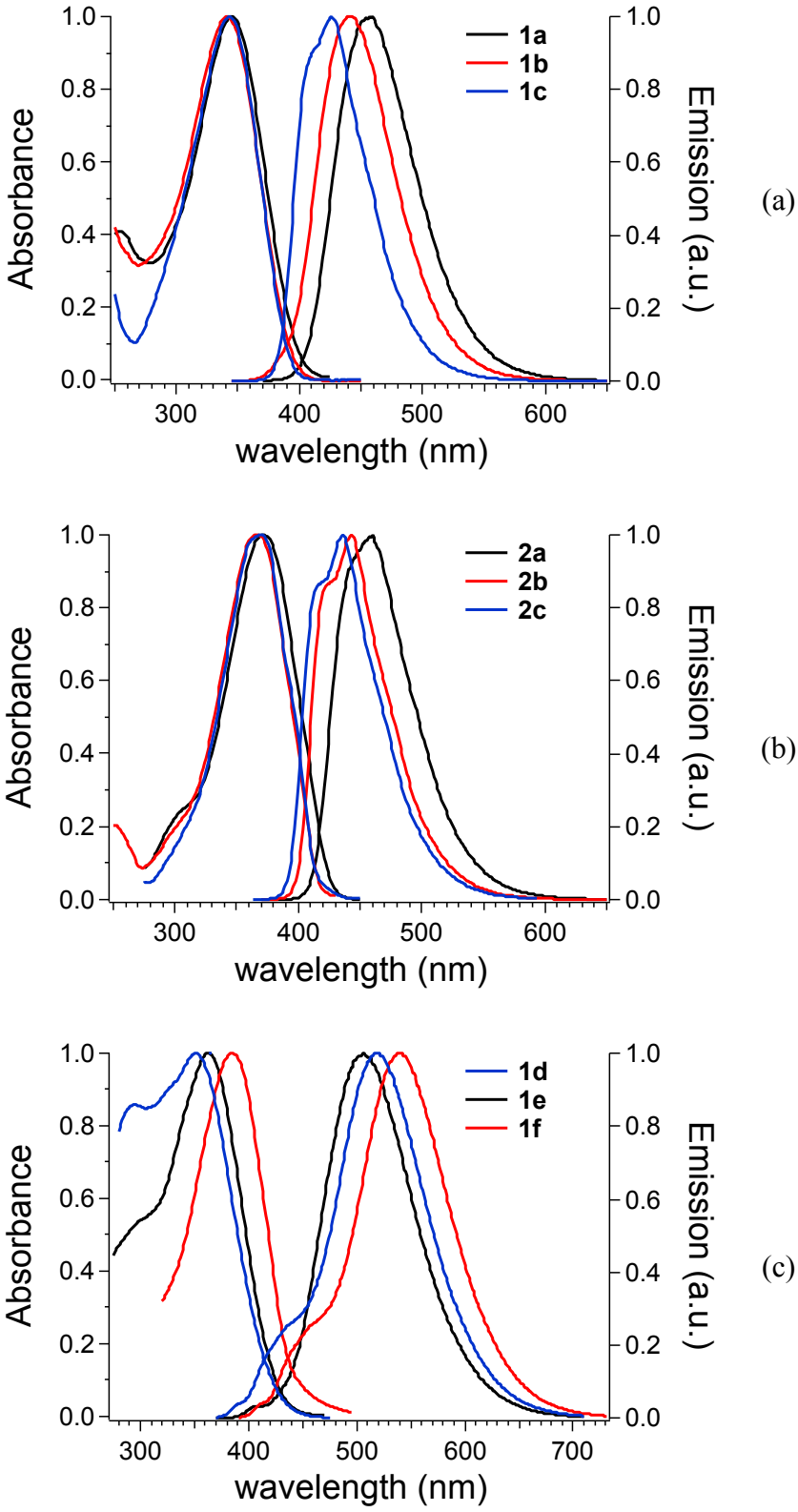

Figure 1. Normalized absorption and emission spectra of 10^{-5} M $CHCl_3$ solutions of **1a-c** ((a), $\lambda_{exc.}$= 330 nm), **2a-c** ((b), $\lambda_{exc.}$= 355 nm) and **1d-f** ((c), $\lambda_{exc.}$= 363 nm)

The same trend was also observed for 1,4-phenylene-spaced thiazole-benzothiazole fluorophores that were prepared aimed primarily at increasing the emission wavelength while maintaining the SS. Notably, the introduction of the thiazole moiety contributed to red-shift the absorption maxima of more than 25 nm for all **2a-c**, but a lower shift resulted in emission (Figure 1b). This behaviour caused the decreasing of SS to less than 80 nm and the significant reduction of Φ below 0.6. Moreover, the emission interval between 436 and 460 nm shown by fluorophores does not match at all the range of maximum efficiency of a photovoltaic cell, thus excluding these fluorophores for final application in luminescent solar concentrators (LSC).[23, 41]

In connection with these findings, 1,4-phenylene-spaced imidazole-benzothiazole **1d-f** were designed with the aim to red-shift their fluorescence emission above 500 nm. Notably, **1e** and **1f** are functionalized at the benzothiazole unit with aldehyde and α-cyano ester electron-withdrawing groups, respectively, whereas **1d** is composed by an electron-donating dimethylamino group. It is worth noting that the introduction of the electron-withdrawing groups red-shifts the emission maximum of 50 (**1e**) and 80 nm (**1f**), respectively, while maintaining the absorption maxima below 390 nm (Figure 1c). This phenomenon contributes to the enhancement in SS to values higher than 140 nm, but adversely affects Φ, whose values were calculated to be 0.50 and 0.11 for **1e** and **1f**, respectively. The very low Φ for **1f** could be possibly attributed to the fact that the higher is the emission wavelength, the lower is the quantum efficiency. Indeed red-emitting organic fluorophores strongly quench their own fluorescence both in solution and in condensed phases.[42]

Compound **1d** was then utilized to achieve a trade-off between longer emission wavelengths and Φ higher than 0.3-0.4, in order to comply with the requirements of fluorophores in LSC.[4] The introduction of the dimethylamino group in the 1,4-phenylene-spaced imidazole-benzothiazole conjugated structure provided an absorption band peaked at 351 nm, a fluorescence maximum at 516 nm (SS = 165 nm) and a Φ higher than 0.4. Moreover, the extinction coefficient was calculated to be similar to the highest reported in Table 1. Notably, the combination of optical properties, i.e.

no significant absorption for wavelengths > 400 nm, largest SS, emission > 500 nm and Φ of 0.42, allowed **1d** to be investigated in PMMA films for applications as colourless LSC.

*Optical characterization of the **1d**/PMMA films*

Owing to the aforementioned opto-electronic properties, **1d** was also investigated when dispersed in the transparent and totally amorphous polymer matrix of PMMA. PMMA is 100% amorphous, transparent, cheap and commercially available, characteristics that make this polymer a perfect candidate for large-scale LSC applications.[43]

The optical characteristics of 0.5 wt.% of **1d** in PMMA films are reported in figure 2 with maximum absorption and emission bands found at 359 nm and 496 nm, respectively, with a SS of 137 nm.

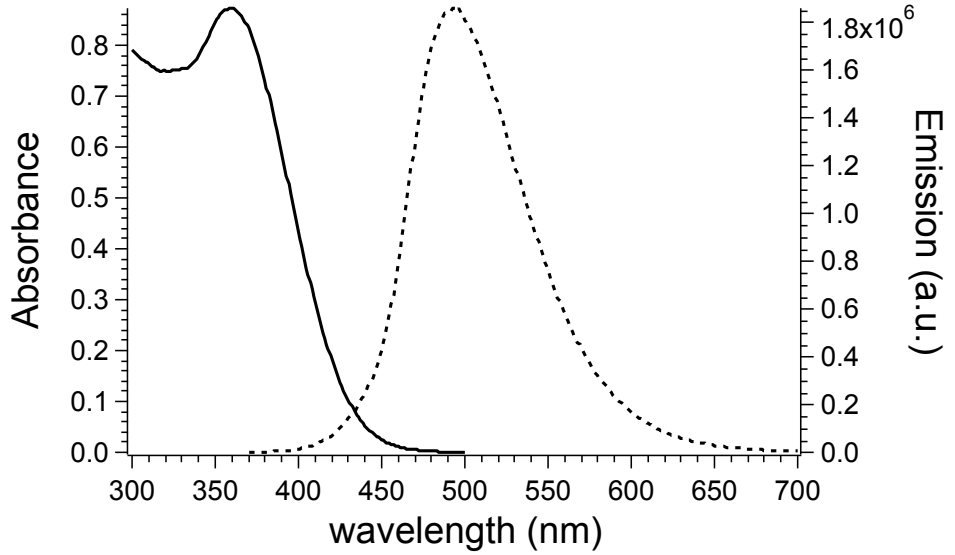

Figure 2. Absorption (solid line) and emission spectra (dotted line, $\lambda_{exc.}$= 360 nm) of a 0.5 wt.% **1d**/PMMA film with a thickness of 25±5 μm.

1d shows absorptions in the near-UV region with a negligible contribution in the visible range of the light spectrum (at 440 nm, about 90% of transmitted light, Figure 3a)) also in the solid state when dispersed in the polymer matrix. SS of **1d** in PMMA is smaller than that recorded in $CHCl_3$ solution, possibly due to the blue-shifted emission caused by the different dielectric constant (for PMMA = 2.6-2.8; for $CHCl_3$ = 4.81). Nevertheless, a SS larger than 135 strongly limits any adverse

auto-absorption phenomena among **1d** fluorophores and contributes to a brilliant green emission from the PMMA film (Figure 3b).

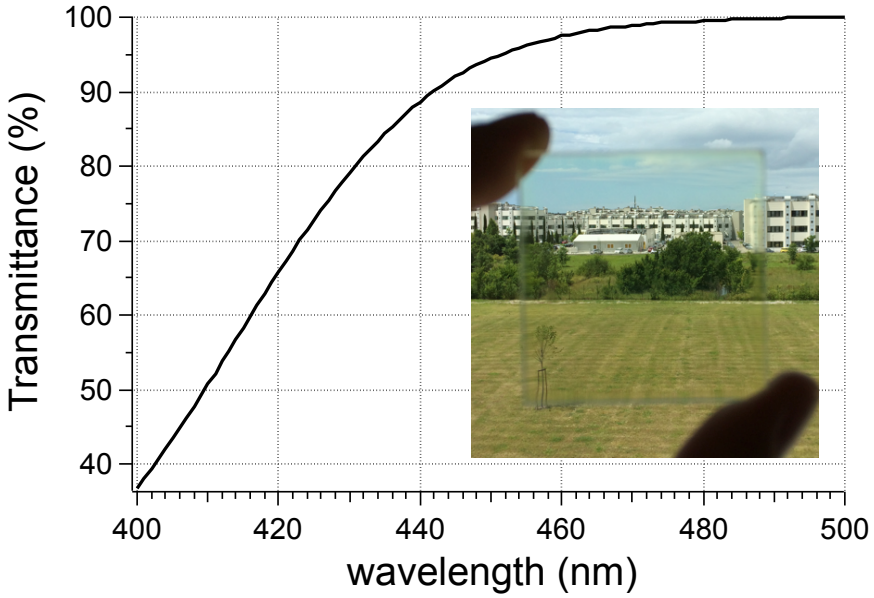

(a)

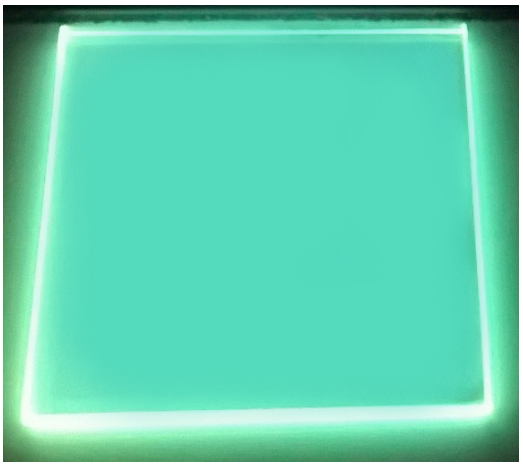

(b)

Figure 3. (a) UV-Vis transmittance spectrum in the 400-500 nm region of a 1.6 wt.% **1d**/PMMA film with a thickness of 25±5 μm coated over an optically pure 50x50x3 mm glass and picture of the same film under (inset) visible light and (b) a long-range UV lamp at 366 nm

The absolute fluorescent quantum yield (QY) of **1d** in PMMA reached an average value of 28 %, which slightly decreased at the highest concentration investigated (i.e. 22 % for 1.8 wt.% **1d**/PMMA film). This value is lower than that of $CHCl_3$ solution (42 %) due to the self-quenching that usually accompanies fluorophores in the solid state,[42] but it results still interesting and promising for optical applications in polymers.

The performances of **1d** PMMA films as LSC were determined on optically pure 50x50x3 mm glass. Photocurrent measurements were accomplished with a home-built apparatus[41] by using a set of three 1x1 cm photodiodes assembled in parallel fashion. Photodiodes are ideal for measuring light sources in LSC emission range by converting the optical power to an electrical current, allowing for a fast, precise and reproducible response even with different sets of samples. This approach was used to study the best working conditions for different **1d**/PMMA films since the response curves of the photodiodes and the utilized PV module do not differ significantly.

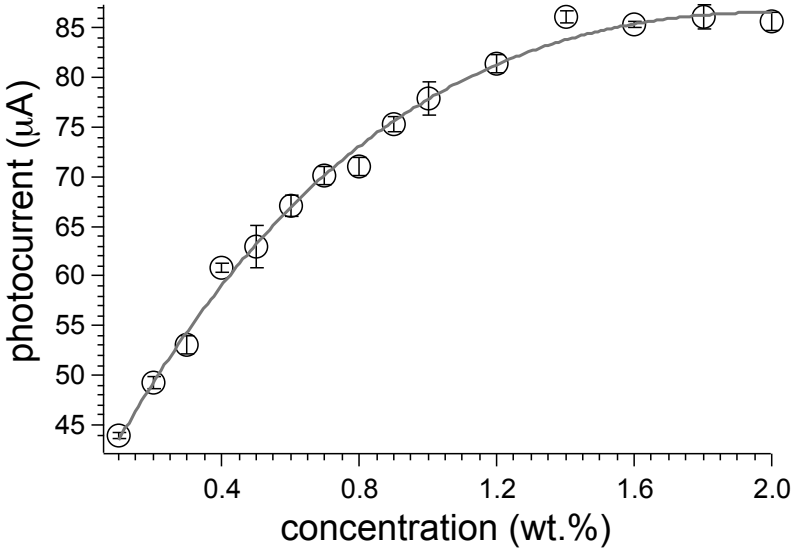

Figure 4. Photocurrent of **1d**/PMMA films of a thickness of 25±5 μm with increasing dye concentration (wt.%). Photocurrents were fitted with eq. 1 (grey curve) with parameters listed in Table 2 (see below)

The data follow a peculiar trend, *i.e.* photocurrent increasing with **1d** content and levelling off at the highest concentration investigated (>1.6 wt.%). In detail, photocurrent is found to increase steadily with **1d** concentration up to 1.4 wt.% of fluorophore, indicating a negligible effect of self-quenching on fluorescence efficiency. Conversely, when the concentration is further increased adverse dissipative phenomena prevail.

Notably, the photocurrent behaviour fits quite well with eq. 1:

$$\eta_{opt} = \varepsilon' \cdot c \cdot e^{-\mu_{opt} \cdot c} + D \qquad \text{(eq.1)}$$

where η_{opt} is the optical efficiency a term proportional to the current generated by photodiodes, c is the concentration of the dye in wt.%, and ε' and μ_{opt} are two empirical constants defined as:

$$\varepsilon' \propto h \cdot e^{-\bar{l}} \qquad \text{(eq. 2)}$$

$$\mu_{opt} \propto \mu''(QY, p) \cdot \bar{l} \qquad \text{(eq. 3)}$$

where h is the thickness of the thin film, $\bar{l}$ is the mean path length of the radiation in the optical system and μ'' is a term depending on both QY and the probability of fluorescence re-absorption (p), being greater at high p and low QY. D is an empirical constant added since even an empty system of transparent material (c = 0) is capable of trapping some light by means of surface and bulk defects due to scattering phenomena.

Eq. 1 was recently determined inspired by the work of Goezberger[5] who proposed in 1977 an effective method to evaluate LSC efficiency. Both ε' and μ_{opt} must be considered as completely empirical since even the most accurate estimations require strong approximations. Nevertheless, the determination of how they affect the final η_{opt} is straightforward for determining the LSC performances. Notably, ε' is a coefficient related to the absorption properties of the dye/polymer system, whereas μ_{opt} combines all the fluorescence quenching mechanisms due to the dye. An optimal dye/polymer system should therefore present a high ε' and a small μ_{opt} so that the maximum efficiency is shifted to higher concentrations and the curve steadily rises under the influence of the linear part (eq. 1). A complete and exhaustive determination of eq. 1 was recently reported in literature by our group.[41]

The fitting parameters, reported in Table 1, were compared to those recently gathered for PMMA films with the same thickness of 25±5 μm but containing Lumogen Red F350 (LR),[41, 44] selected as reference as it is considered the state-of-the-art for LSC applications.[4]

Table 2. Fitting parameters of the photocurrent data measured for **1d**/PMMA and LR/PMMA[41] films. For both systems, the film thickness was 25±5 μm

Entry	ε'	μ_{opt}	D
1d/PMMA	67	0.49	35
LR/PMMA	140	0.45	20

The fitting parameters of **1d**/PMMA films were found to be different from those of LR/PMMA only for ε'. The smaller ε' is a result of the lesser absorption window of **1d** compared to that of LR in PMMA, being ε' related to the light absorption properties of the system. This data is not surprising since **1d** was actually designed to have limited absorption in the visible region of light spectrum. It is worth noting that the fluorophores showed identical μ_{opt} values, notwithstanding the lower QY of **1d** compared to that of LR (28% against about 1, respectively).[41] This phenomenon is possibly ascribed to the limited fluorescence quenching mechanisms experienced by **1d** at high concentration, which confer PMMA films excellent emission efficiencies. Moreover, D values resulted to be quite similar for all the dye/PMMA systems, thus suggesting that the contribution of non–fluorescent trapping is more or less the same for samples with the same thickness.

The **1d**/PMMA films with the highest photocurrent, i.e. the those containing the 1.4 and 1.8 wt.% of **1d**, were analysed by using a Si-based PV cell attached to one edge of the concentrator, as described in the experimental section. The optical efficiency η_{opt} (Table 3) was evaluated from the concentration factor C, which is the ratio between the short circuit current measured in the case of the cell over the LSC edge (I_{LSC}) and short circuit current of the bare cell when perpendicular to the light source (I_{SC}) (eq. 4):

$$\eta_{opt} = \frac{I_{LSC}}{I_{SC} \cdot G} \quad \text{(eq. 4)}$$

where G is the geometrical factor (in our case, G = 13.3), which is the ratio between the area exposed to the light source and the collecting area.

Table 2. Optical efficiencies (η_{opt}) calculated for **1d**/PMMA LSC and compared to those of LR/PMMA LSC with similar geometrical factor[9, 41]

Entry	**wt.%**	**η_{opt} (%)**
1d/PMMA	1.4	5.2
	1.6	5.3
	1.8	5.9
LR/PMMA	1.5-1.8	~8.0

The calculated η_{opt} for the **1d**/PMMA system with the highest photocurrents was not surprisingly found lower than that gathered from LSC based on LR in the same range of fluorophore concentration and geometrical factor. The difference of about 2% between optical efficiencies is a result of the poor visible light absorption by **1d** fluorophores compared to the state-of-the-art LR. Nevertheless, it is worth mentioning that η_{opt} reached values as high as 6%, possibly thanks to the large SS (i.e., 137 nm for **1d**/PMMA and 23 nm for LR/PMMA[44]) that strongly contributes in limiting fluorescence quenching, thus fostering its concentration.

Conclusions

We have shown that the dispersion of a near-UV absorbing imidazole-benzothiazole fluorophore with brilliant green emission in PMMA allowed the preparation of thin film LSC with a faint colored tinting and optical efficiencies close to 6.

Different fluorophores characterized by imidazole-benzothiazole and thiazole-benzothiazole backbones were synthesized aimed at obtaining the best combination of optical properties in terms of near-UV absorption, Stokes shift larger than 150 nm and a fluorescence quantum yield higher than 0.4. Among them, the 1,4-phenylene-spaced imidazole-benzothiazole bearing an electron-donating dimethylamino group was found the best candidate and was selected as fluorescent dopant in PMMA thin films. Photocurrent experiments of the derived LSC revealed optical efficiencies not surprisingly lower than those evaluated by the state-of-the-art systems due to the limited absorption in the visible region. Nevertheless, η_{opt} values as high as 6 flanked by significant light transmittance in the visible region consistently support the use of the prepared device in the realization of colourless LSC.

Acknowledgements

The research leading to these results has received funding from MIUR-FIRB (RBFR122HFZ) and in part from the Università di Pisa under PRA 2015 (project No. 2015_0038).

References

[1] Debije M. Renewable energy Better luminescent solar panels in prospect. Nature. 2015;519(7543):298-9.
[2] Sawin JL. Renewables Global Status Report. Renewable Energy Policy Network for the 21th Century. Renewable Energy Policy Network for the 21th Century ed. Paris: Renewable Energy Policy Network for the 21th Century; 2014.
[3] van Sark WGJHM. Luminescent solar concentrators - A low cost photovoltaics alternative. Renewable Energy. 2013;49(0):207-10.
[4] Debije MG, Verbunt PPC. Thirty Years of Luminescent Solar Concentrator Research: Solar Energy for the Built Environment. Advanced Energy Materials. 2012;2(1):12-35.
[5] Goetzberger A, Greube W. Solar energy conversion with fluorescent collectors. Appl Phys. 1977;14(2):123-39.
[6] Turrisi R, Sanguineti A, Sassi M, Savoie B, Takai A, Patriarca GE, et al. Stokes shift/emission efficiency trade-off in donor-acceptor perylenemonoimides for luminescent solar concentrators. Journal of Materials Chemistry A: Materials for Energy and Sustainability. 2015;3(15):8045-54.
[7] Meinardi F, Colombo A, Velizhanin KA, Simonutti R, Lorenzon M, Beverina L, et al. Large-area luminescent solar concentrators based on 'Stokes-shift-engineered' nanocrystals in a mass-polymerized PMMA matrix. Nature Photonics. 2014;8(5):392-9.
[8] Sanguineti A, Sassi M, Turrisi R, Ruffo R, Vaccaro G, Meinardi F, et al. High Stokes shift perylene dyes for luminescent solar concentrators. Chemical Communications. 2013;49(16):1618-20.
[9] Griffini G, Levi M, Turri S. Thin-film luminescent solar concentrators: A device study towards rational design. Renewable Energy. 2015;78:288-94.
[10] Zhao Y, Meek GA, Levine BG, Lunt RR. Near-Infrared Harvesting Transparent Luminescent Solar Concentrators. Advanced Optical Materials. 2014;2(7):606-11.
[11] Benjamin WE, Veit DR, Perkins MJ, Bain E, Scharnhorst K, McDowall S, et al. Sterically Engineered Perylene Dyes for High Efficiency Oriented Fluorophore Luminescent Solar Concentrators. Chemistry of Materials. 2014;26(3):1291-3.
[12] Currie MJ, Mapel JK, Heidel TD, Goffri S, Baldo MA. High-Efficiency Organic Solar Concentrators for Photovoltaics. Science. 2008;321(5886):226-8.
[13] Daorta SF, Liscidini M, Andreani LC, Scudo P, Fusco R. THEORETICAL STUDY OF MULTILAYER LUMINESCENT SOLAR CONCENTRATORS USING A MONTE CARLO APPROACH. 26th European Photovoltaic Solar Energy Conference and Exhibition. Hamburg2011.
[14] Desmet L, Ras AJM, de Boer DKG, Debije MG. Monocrystalline silicon photovoltaic luminescent solar concentrator with 4.2% power conversion efficiency. Opt Lett. 2012;37(15):3087-9.
[15] Goldschmidt JC, Peters M, Bosch A, Helmers H, Dimroth F, Glunz SW, et al. Increasing the efficiency of fluorescent concentrator systems. Solar Energy Materials and Solar Cells. 2009;93(2):176-82.
[16] Slooff LH, Bende EE, Burgers AR, Budel T, Pravettoni M, Kenny RP, et al. A luminescent solar concentrator with 7.1% power conversion efficiency. physica status solidi (RRL) – Rapid Research Letters. 2008;2(6):257-9.

[17] Bailey ST, Lokey GE, Hanes MS, Shearer JDM, McLafferty JB, Beaumont GT, et al. Optimized excitation energy transfer in a three-dye luminescent solar concentrator. Solar Energy Materials and Solar Cells. 2007;91(1):67-75.
[18] Flores Daorta S, Proto A, Fusco R, Claudio Andreani L, Liscidini M. Cascade luminescent solar concentrators. Applied Physics Letters. 2014;104(15):-.
[19] Balaban B, Doshay S, Osborn M, Rodriguez Y, Carter SA. The role of FRET in solar concentrator efficiency and color tunability. Journal of Luminescence. 2014;146:256-62.
[20] Beverina L, Sanguineti A. Organic fluorophores for luminescent solar concentrators. Solar Cell Nanotechnology. 2014:317-55.
[21] Al-Kaysi RO, Sang Ahn T, Muller AM, Bardeen CJ. The photophysical properties of chromophores at high (100 mM and above) concentrations in polymers and as neat solids. Physical Chemistry Chemical Physics. 2006;8(29):3453-9.
[22] Reisfeld R, Shamrakov D, Jorgensen C. Photostable solar concentrators based on fluorescent glass films. Solar Energy Materials and Solar Cells. 1994;33(4):417-27.
[23] Carlotti M, Ruggeri G, Bellina F, Pucci A. Enhancing optical efficiency of thin-film luminescent solar concentrators by combining energy transfer and stacked design. Journal of Luminescence. 2016;171:215-20.
[24] Lessi M, Manzini C, Minei P, Perego LA, Bloino J, Egidi F, et al. Synthesis and Optical Properties of Imidazole-Based Fluorophores having High Quantum Yields. ChemPlusChem. 2014;79:366-70.
[25] Bellina F, Lessi M, Manzini C. Mild Palladium-Catalyzed Regioselective Direct Arylation of Azoles Promoted by Tetrabutylammonium Acetate. European Journal of Organic Chemistry. 2013;2013(25):5621-30.
[26] Bellina F, Cauteruccio S, Di Fiore A, Rossi R. Regioselective Synthesis of 4,5-Diaryl-1-methyl-1H-imidazoles Including Highly Cytotoxic Derivatives by Pd-Catalyzed Direct C-5 Arylation of 1-Methyl-1H-imidazole with Aryl Bromides. European Journal of Organic Chemistry. 2008;2008(32):5436-45.
[27] Roger J, Doucet H. Phosphine-free palladium-catalysed direct 5-arylation of imidazole derivatives at low catalyst loading. Tetrahedron. 2009;65(47):9772-81.
[28] Primas N, Bouillon A, Lancelot J-C, El-Kashef H, Rault S. Synthesis of 5-arylthiazoles. Comparative study between Suzuki cross-coupling reaction and direct arylation. Tetrahedron. 2009;65(29–30):5739-46.
[29] Jensen J, Skajærbæk P, P. V. Preparation of 2- and 5-Aryl Substituted Thiazoles via Palladium-Catalyzed Negishi Cross-Coupling. Synthesis. 2001:128-34.
[30] Roger J, Požgan F, Doucet H. Ligand-Free Palladium-Catalyzed Direct Arylation of Thiazoles at Low Catalyst Loadings. The Journal of Organic Chemistry. 2009;74(3):1179-86.
[31] Chen L, Yang C, Li S, Qin J. Synthesis and electronic absorption and fluorescence of 2-arylbenzothiazole derivatives. Spectrochimica Acta Part A: Molecular and Biomolecular Spectroscopy. 2007;68(2):317-22.
[32] Wang H, Chen G, Xu X, Chen H, Ji S. The synthesis and optical properties of benzothiazole-based derivatives with various π-electron donors as novel bipolar fluorescent compounds. Dyes and Pigments. 2010;86(3):238-48.
[33] Kalwania GS, Chomal S, Choudhary S. Facile Synthesis of Bioactive 4H-[1,4]-Benzothiazines Under Solvent Free Conditions. Asian J Chem. 2011;23:5133-6.
[34] Weekes AA, Bagley MC, Westwell AD. An efficient synthetic route to biologically relevant 2-phenylbenzothiazoles substituted on the benzothiazole ring. Tetrahedron. 2011;67(40):7743-7.
[35] Bellina F, Cauteruccio S, Mannina L, Rossi R, Viel S. Regiocontrolled Synthesis of 1,2-Diaryl-1H-imidazoles by Palladium- and Copper-Mediated Direct Coupling of 1-Aryl-1H-imidazoles with Aryl Halides under Ligandless Conditions. European Journal of Organic Chemistry. 2006;2006(3):693-703.

[36] Bellina F, Calandri C, Cauteruccio S, Rossi R. Efficient and highly regioselective direct C-2 arylation of azoles, including free (NH)-imidazole, -benzimidazole and -indole, with aryl halides. Tetrahedron. 2007;63(9):1970-80.
[37] Bellina F, Cauteruccio S, Di Fiore A, Marchetti C, Rossi R. Highly selective synthesis of 4(5)-aryl-, 2,4(5)-diaryl-, and 4,5-diaryl-1H-imidazoles via Pd-catalyzed direct C-5 arylation of 1-benzyl-1H-imidazole. Tetrahedron. 2008;64(26):6060-72.
[38] Heravi MM, Tehrani MH, Bakhtiari K, Oskooie HA. A practical Knoevenagel condensation catalysed by imidazole. Journal of Chemical Research. 2006;9:561-2.
[39] Brouwer AM. Standards for photoluminescence quantum yield measurements in solution (IUPAC Technical Report). Pure and Applied Chemistry. 2011;83(12):2213-28.
[40] Lide D, Haynes W. CRC handbook of chemistry and physics: a ready-reference book of chemical and physical data-/editor-in-chief, David R. Lide; ass. ed. WM" Mickey" Haunes: Boca Raton, Fla: CRC, 2009.
[41] Carlotti M, Panniello A, Fanizza E, Pucci A. A Fast and Effective Procedure for the Optical Efficiency Determination of Luminescent Solar Concentrators. Solar Energy. 2015;119:452-60.
[42] Valeur B, Berberan-Santos MN. Molecular Fluorescence: Principles and Applications. second ed. Weinheim (Germany): Wiley-VCH, 2013.
[43] Sperling LH. Introduction to Physical Polymer Science. 4th ed. Hoboken, New Jersey: John Wiley & Sons, Inc., 2006.
[44] Pucci A, Pavone M, Minei P, Munoz-Garcia AB, Fanizza E, Cimino P, et al. Cost-effective Solar Concentrators based on Red Fluorescent Zn(II)-Salicylaldiminato Complex. RSC Advances. 2016;6:17474-82.

Graphical abstract